

Use of UAV-Based RGB Imagery and Vegetation Index for Early Detection of the Rabies of Chickpeas

Lorena Parra^{1,2}, Barbara Stefanutti, David Mostaza-Colado¹, Jose F. Marin³, Jaime Lloret², and Pedro V. Mauri¹

¹Instituto Madrileño de Investigación y Desarrollo Rural, Agrario y Alimentario (IMIDRA), Finca “El Encin”, A-2, Km 38, 2, 28805 Alcalá de Henares, Madrid, Spain

²Instituto de Investigación para la Gestión Integrada de Zonas Costeras Universitat Politècnica de València, Valencia, Spain

³Area verde MG Projects SL. C/ Oña, 43 28933 Madrid, Spain

Email: loparbo@doctor.upv.es, barbara.stefanutti@madrid.org, david.mostaza@madrid.org, jmarin@areaverde.es, jlloret@dc.com.upv.es, and pedro.mauri@madrid.org

Abstract—Rainfed crops rarely include the application of phytosanitary products due to the high cost of their application and the reduced rentability of crops. Nonetheless, if diseases are early detected, phytosanitary application costs are heavily reduced. This paper presents a method of detecting rabies in chickpeas based on true-colour images gathered from drones. The methodology consists of applying a series of vegetation indexes and filters. In the proposed method, applied to several images, we include the detection of areas affected by rabies of chickpea but also their differentiation from other areas with lower vigour. The developed approach is tested with images obtained in different soil types and gathered at diverse flying heights. As vegetation indexes, we used well-known vegetation indexes and specific vegetation indexes developed for chickpeas. To evaluate the accuracy of the proposed methodology, the number and percentage of true positives and false positives are assessed. Moreover, a verification is done using a different picture in order to evaluate if the methodology might be applied in other scenarios. The results of the initial test and the verification test offer a number of true positives higher than 85%. Thus, we can affirm that the proposed methodology can be useful for the differentiation between areas affected by rabies of chickpea and areas with low vigour due to the passing of machinery.

Keywords—plant disease; aggregation; image processing; legume; biotic stress; crop

I. INTRODUCTION

Chickpea is a legume crop with a high percentage of protein, which can help to reduce the dependence on meat. Spain is the main producer of chickpea in Europe. Nonetheless, the cultivation of chickpeas has declined in recent decades. As indicated by the Lonja de Sevilla, the main problems are the following: (i) Lack of support via Common Agrarian Policy, (ii) Little Research (little use of certified seed), (iii) Technical difficulties in crop management (high presence of weeds, diseases, such as rabies and harvesting problems) and (iv) Obstacles in marketing. The technical difficulties of crop management are the most important for farmers and those that can be solved by means of new technologies. Of these difficulties, the detection of weeds [1] and plants affected by diseases [2] are vital in chickpea cultivation and other crops. Among the chickpea diseases,

rabies of the chickpea is one of the most problematic ones, causing a decrease in production and even the death of the plant.

The use of a remote sensing approach is pointed out as one of the best methodologies for evaluating plant features. In other crops, the use of remote sensing for detecting plant diseases is common. According to [3], the most studied diseases are fungal diseases. They are generally studied in cereals such as wheat, rice and maize, followed by soya. No study evaluated the use of hyperspectral images in chickpeas or other rainfed legumes. In [4], a large collection of Vegetation Indexes (VI) developed by different authors for diverse crops is presented. The authors indicate that VI are highly correlated at plot level with the presence of plant diseases. Focusing on VI, RGB images are reported as adequate for cotton, sugar beet, grapefruit, and tobacco [5]. Although hyperspectral images provide more information than RGB images, the elevated cost of hyperspectral cameras precludes its use for real solutions.

The main problem of applying VI to identify the areas to be treated is that we can find other zones characterised by low vigour in the fields, which can be confused with zones affected by rabies. These zones are usually the areas that have been stepped on by a tractor when entering to apply treatments. If the areas are not correctly differentiated, phytosanitary products will be wasted, increasing the treatment's cost and efficiency.

The aim of this paper is to evaluate the use of RGB images taken by Unmanned Aerial Vehicle (UAV) to identify areas affected by rabies in different fields. The images have been taken at different heights and included affected and unaffected areas. The entire process includes the application of the VI (testing up to 5 different VI) and the use of different tools for image processing, such as aggregation or reclassification tools. Simple tools are selected to avoid the use of artificial intelligence or complex tools. This, ensures that the methodology can be applied in the fields in real time. Thus, the Unmanned Aerial Vehicle (UAV) will be able to identify the areas to be treated and apply the treatment at the same time.

The rest of the paper is structured as follows; Section II outline the related work and the gap in the current solutions. The proposal is described in Section III. Section IV details the material and methods used in this research. The results and

main discussion are presented in Section V. Finally, the conclusion and future work are summarised in Section VI.

II. RELATED WORK

This section summarises the existing proposals for identifying diseases or abiotic stress in plants using RGB images and the existing VI developed for chickpeas.

Regarding the use of RGB images to identify plant diseases, we can find a limited number of examples. More examples of using the RGB data to evaluate abiotic stress.

In 2019, Marc Sancho-Adamson et al. [6], showed the use of RGB-based VI for evaluating the effects of VerticilliumWilt of olive. The authors used the following VI: Green Area (GA), Greener Area (GGA), normalised green-red difference index and triangular greenness index. Their results indicate that GA was the one with the strongest correlations between the VI and chlorophyll and carotenoid extractions to identify the diseases. Nonetheless, the VI was applied in pictures done in the laboratory, not in the field.

Another example of the application of RGB indexes to identify plant diseases was published in 2021 by Arturo Yee-Rendon [7]. In their paper, the authors pointed out the possibility of using RGB-based VI for detecting tobacco mosaic virus and pepper huasteco yellow vein Virus in jalapeño pepper plants. New VI was proposed and evaluated. The authors combine the VI with a convolutional neural network to identify the affected leaves in their proposal. Their results indicate that the VI with better accuracy was the normalised green-blue vegetation index, which combines the green and the blue bands.

In 2021, Brenon Diennevam Souza Barbosa et al. [8], assess the use of RGB images for monitoring a coffee farm. A total of 9 VI were used and correlated with the obtained Leaf Area Index (LAI). Results indicate that the index that best correlates with the LAI varies along the different phenological stages of the crop. Salima Yousfi et al. in 2022 [9] present the use of RGB-based VI for evaluating the hydric stress in turfgrasses. GA and GGA were used to assess the stress of the plants. Their results indicate that RGB-based VI obtained from aerial images explains the hydric stress of the plants better than terrestrial indexes, even better than the Normalised Difference Vegetation Index (NDVI). The NDVI is a well-known VI that uses not only the RGB data but also the information of infrared light.

Finally, a few examples of VI applied for chickpeas monitoring can be found. Particularly, in the case of RGB indexes, only two papers have been published. In the first example, the VI was used to differentiate soil from vegetation in order to assess the degree of establishment of different legumes, including lentils and chickpea [10]. In the second example, a tailored VI including a series of thresholds is used to differentiate species of legumes in intercropping. The included species were chickpea, lentil and ervil. The results of [11] pointed out that chickpea was the species that was easier to differentiate.

As far as we know, no paper has shown the use of RGB-based VI to identify chickpea's rabies nor to differentiate regions affected by the disease and the pass of machinery. Moreover, no example of RGB-based VI applied in the field

is found. Thus, the methodology presented in this paper can be considered an advance over state of the art.

III. PROPOSAL

In this section, we outline the proposal developed in the paper. We will describe why the proposed methodology is the most suitable approach for the problem.

The problem indicated in the introduction is differentiating areas affected by rabies of chickpea from areas with lower vigour due to the passing of machinery. Our proposal is to develop a methodology that allows an UAV to apply it in real-time to smartly decide the areas to be treated with the phytosanitary product. The aim is to minimise the application of phytosanitary products treating only the area affected by the disease and its surroundings. Thus, it is essential to differentiate the areas in which crop has low vigour due to the rabies of the chickpea from the areas with low vigour due to the machinery, which does not need any treatment.

Figure 1 shows an example of a picture in which, manually, we have differentiated the areas with low vigour and their cause. The proposed approach is depicted in Figure 2, in which we represent the whole process to minimise the use of phytosanitary products. Applying the phytosanitary product to the affected area it is possible to reduce the cost and environmental impact of the treatment without minimizing its effectivity. Traditionally, the phytosanitary product is applied to the whole plot.

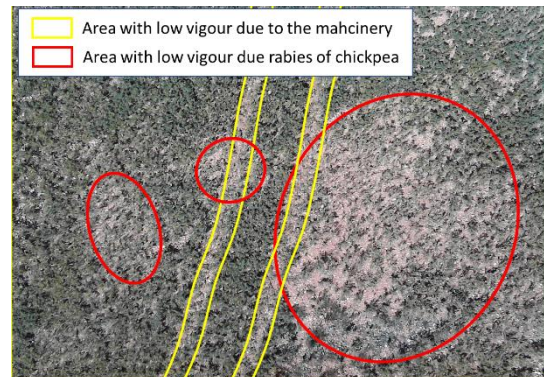


Figure 1. Example of areas with low vigour.

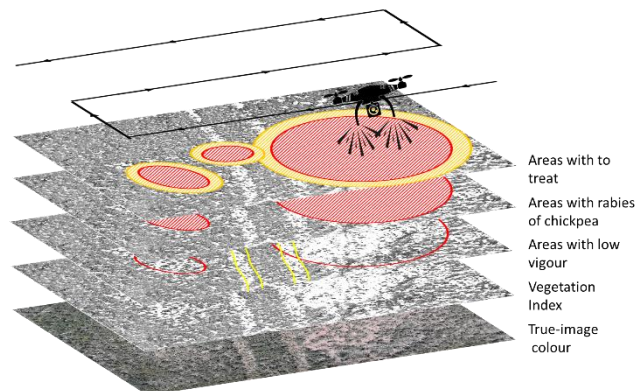


Figure 2. Representation of proposal.

IV. MATERIAL AND METHODS

A. Studied area

The study area is located in the autonomous community of Castilla la Mancha (Spain), in the municipality of Trijueque (40°46'45"N, 2°59'2"W) at an approximate altitude of 1,000 m.a.s.l. The location of the studied area in Spain and the detailed image of the studied fields can be seen in Figure 3 a) and Figure 3 b). The studied area is composed of two production fields in which chickpea is grown. Different crop densities characterise the plots due to different soils. Plots are located on a plain close to a highway.

Pictures were gathered on 25 May 2021 in cloudless sky conditions (clouds covered less than 20% of the sky). This ensures the light condition for picture collection.

B. Studied crop

In the studied plots, chickpeas are in the reproductive stage. More specifically, chickpea was in the phenologic state R6, with the seeds starting their formation in the pods. The plants have an approximate height of about 40 cm. The plots belong to a variety of chickpea with small seeds.

At different points of the plots, it is possible to identify areas affected by rabies of chickpeas. Those areas can be seen in Figure 4. In addition to the affected areas, the use of agricultural machinery in the early stages has affected the correct development of plants.

C. AUV details

The images are taken by a drone (Parrot Bebop 2) that uses an RGB and thermal camera (FLIR ONE Pro thermal – RGB camera). In the present study, only the information from the RGB camera is used. Figure 5 depicts the data gathering process.

Figure 3. Location of the studied area, a) location in the Iberian Peninsula and b) image of the fields.



Figure 4. Terrestrial picture of the studied area.



Figure 5. Picture during data collection.

D. Image processing

The pictures were taken at a height of 8 to 10 m above the ground. The images are subsequently processed mathematically to identify the areas with low vigour, differentiating the areas affected by rabies from the areas affected by the passage of a tractor. In Figure 1, we can see an example of the images taken. In each of the images, the tractor pass (on the left of the image) and the area affected by rabies (on the right of the image) are identified.

The problem that we need to solve is the possible false positives caused by the tractor tread area. It is expected that when applying the VI, both the areas affected by rabies and the areas trampled by the tractor will give similar results.

The process used with the images to identify areas with low vigour and differences between areas affected by rabies or by the passage of a tractor is broken down into the following elements: (i) Application of the VI (created for this case), (ii) Tools to differentiate false positives from the machinery pass, and (iii) Aggregation techniques and mathematical operations between bands. The process is summarized in Figure 6.



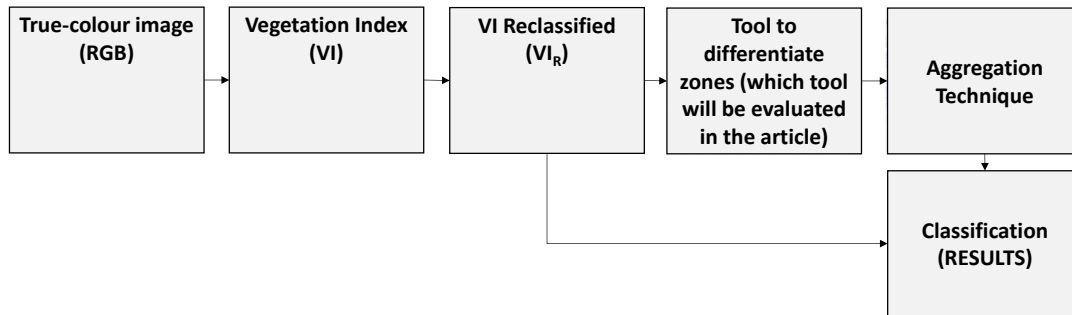


Figure 6. Block diagram of the followed process, including the most relevant tools (VI, reclassification and aggregation technique).

V. EVALUATION OF RESULTS AND DISCUSSION

In this section, we analyse the results of the proposed methodology and the selected values for each of the conducted steps. Moreover, we display the code of the used tools.

A. Followed process

Figure 7 shows the results of the processes followed to identify the areas affected by rabies. An example of the raster obtained working with the image taken at 10 m is shown in each block diagram.

As VI, we have evaluated the use of well-known VI as well as analysed the generation of tailored VI. The use of existing VI does not offer good results compared with the proposed VI. Among the proposed VI, five different VI were considered. Being the VI indicated in (1), the one with better results. Three of the proposed VI are based on blue and green bands (B3 and B2), another VI is based on red and green bands (B1 and B2), and the last one on the three bands (B1, B2 and

B3). The VI with better results is the one based on the combination of the three bands.

Another relevant finding of this paper is that the "Thin" tool was the one that allowed the differentiation of the areas with low vigour due to the machinery from the areas affected by rabies of chickpea. The differentiation is done based on the different shapes of affected areas (round for rabies of chickpea and linear for the machinery). This tool was selected among different spatial analyst tools. Other tools tested in this paper included Boundary clean, Expand, Nibble, and Shrink. Nonetheless, none of these tools has proven to be as accurate as of the Thin tool.

We can identify it at the end of the block diagram. As a result, a raster in which combines the AIVR and ATIVRR (see (2)), the red spots indicate the area in which rabies of chickpea appear. The area in grey is discarded due to the fine tool since it indicates that the shape of the area cannot be considered as an area affected by rabies of the chickpea for the given flying height and camera.

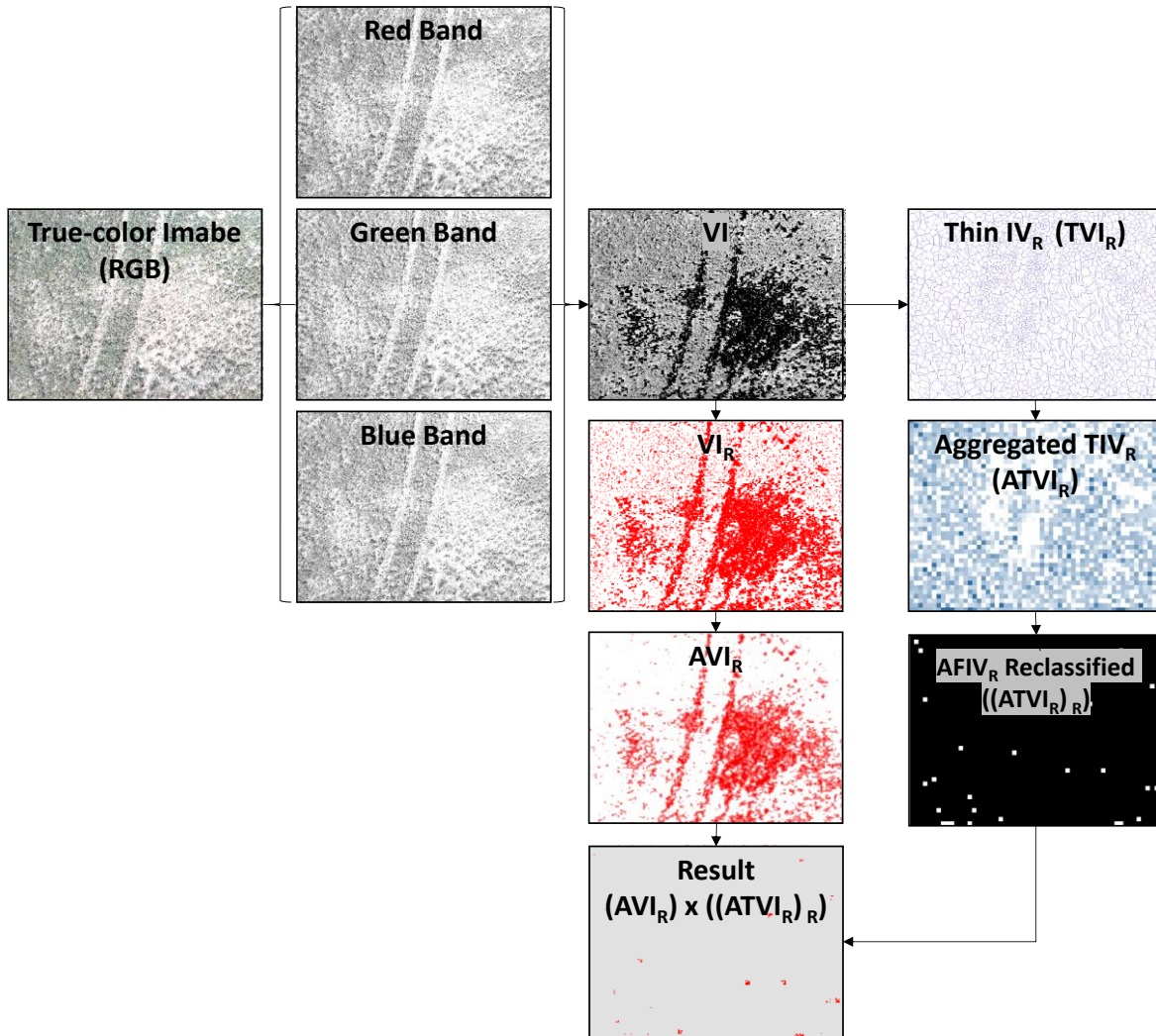


Figure 7. Results of each step until reaching the result.

B. Code and values for selected code

Following the process described in Figure 7, we detail the included code. The first code to be described is used for the reclassification of VI to generate the VIR. This code can be seen in Figure 8. The selected ranges do not need to be adapted if the proposed methodology is applied under different conditions.

In the next step, the use of the Thin tool is defined in Figure 9. In this case, the selected parameters were round since the results are more accurate than with sharp and 50 as the maximum thickness in pixels. The number of maximum thickness should be reconsidered for other scenarios in which the pixel size changes, such as for using another flying height or a camera with a different resolution.

The Aggregation processes for both IVR and ATVIR are defined in Figure 10. The aggregation method (mean for IVR and summation for ATVIR) should not be modified. Nonetheless, the cell size should be reconsidered and adapted for other scenarios.

```

Code 1
# Code for Reclassify Operation (I)
import arcpy
from arcpy import env
from arcpy.sa import *
env.workspace = "C:/sapyexamples/data"
outReclass1 = Reclassify("VI", "Value",
RemapRange([[0,1,1],[1,255,2]]))
outReclass1.save("C:/sapyexamples/output/VIR")
    
```

Figure 8. Code for reclassify operation (i)

```

Code 2:
# Code for Thin
import arcpy
from arcpy import env
from arcpy.sa import *
env.workspace = "C:/sapyexamples/data"
thinOut = Thin("VIR","ZERO", "FILTER", "ROUND",50)
thinOut.save("c:/sapyexamples/output/FIVR")
    
```

Figure 9. Code for thin operation

```

Code 3:
# Code for Aggregate Operation
import arcpy
from arcpy import env
from arcpy.sa import *
env.workspace = "C:/sapyexamples/data"
outAggreg = Aggregate("IVR", 5, "MEAN",
"TRUNCATE", "DATA")
outAggreg.save("C:/sapyexamples/output/AVIR")
outAggreg = Aggregate("TAVIR", 25, "SUMMATION",
"TRUNCATE", "DATA")
outAggreg.save("C:/sapyexamples/output/ATAVIR")
    
```

Figure 10. Code for Aggregate Operation

Finally, Figure 11 presents the reclassification of ATVIR. Again, no modification of this code is needed for different scenarios. The selected values for the aggregation are the ones that allow the assignment of pixel value = 1 in the result of the methodology when the area has rabies of chickpea.

```

Code 4:
# Code for Reclassify Operation (II)
import arcpy
from arcpy import env
from arcpy.sa import *
env.workspace = "C:/sapyexamples/data"
outReclass1 = Reclassify("AFIVR", "Value",
RemapRange([[0,1],[0,255,0]]))
outReclass1.save("C:/sapyexamples/output/VIR")
    
```

Figure 11. Code for reclassify operation (ii).

(1)

(2)

C. Accuracy of obtained results and verification

The proposed methodology makes it possible to identify the areas affected by rabies in 100% of the cases. After removing the positives that are on the edge of the photograph, there are 85.7% true positives versus 14.3% false positives. In the verification of the methodology, using a different picture, we identify 100% of affected areas by rabies of chickpea. In this case, we have 88.2% of true positives and 11.8% of false positives. The results in terms of true positives and false positives are summarised in Table 1.

TABLE I. SUMMARY OF RESULTS AND VERIFICATION

	Accuracy		
	N° of positive pixels	True positives	False positives
Test	7	6 (85.7 %)	1 (14.3 %)

	Accuracy		
	N° of positive pixels	True positives	False positives
Verification	17	15 (88.2 %)	2 (11.8 %)

A correct classification percentage of 80% is within what is expected in this type of case, especially for preliminary results [11]. The precision is lower than in other articles in which more advanced classification techniques are used, in which case the precision is close to 90% [12]. There are cases in which these advanced classification techniques have a precision of less than 80% [13].

D. Discussion

The obtained accuracy, in the verification is aligned with accuracies found in other similar models [10 and 11].

Existing approaches to solve the identification of fungic diseases focused on machine learning are designed for other crops such as cotton [14], wheat [15], maize [16], oilseed rape [17] or strawberry [18], among others. Nonetheless, it is not possible to fairly compare the results since the accuracy of the methodologies are calculated in a wide range of forms (confusion matrices, R2 of the correlation, etc).

Only one paper has been found in which the detection of fungic disease in chickpea is analyzed [19] Nevertheless, in [19] the authors do not offer the accuracy of the disease detection, results are referred to productivity. Another example of use of remote sensing in chickpea, aimed to detect water stress, obtained accuracies between 72 % and 83 %. In a posterior study, using convolutional neural network [21], the maximum accuracy reached 96%. The accuracy of proposed method is aligned with existing accuracies in proposals for chickpea.

The main limitation of the proposed methodology is the use of RGB images. Probably, if infrared information included the differentiation will be easier. However, to maintain the methodology as simple as possible and to avoid using high-cost resources, RGB images are the sole information source.

VI. CONCLUSION

In the presented work, we have evaluated a methodology to identify areas affected by rabies capable of not giving false positives in the areas through which agricultural machinery has passed. It is a preliminary methodology that will be evaluated within the framework of the GO TecnoGAR and Valvagar-Dron Guardes projects in the years 2022 and 2023.

In the future, it is hoped that this information will be combined with specific treatments that will reduce the number of phytosanitary products used to treat large areas. Similar methodologies will also be used to identify weeds.

ACKNOWLEDGMENT

This research was partially funded by the “Programa Estatal de I+D+i Orientada a los Retos de la Sociedad, en el marco del Plan Estatal de Investigación Científica y Técnica y de Innovación 2017–2020” (Project code: PID2020-114467RR-C31 and PID2020-114467RR-C33), and by

“Proyectos de innovación de interés general por grupos operativos de la Asociación Europea para la Innovación en materia de productividad y sostenibilidad agrícolas (AEI-Agri)” in the framework “Programa Nacional de Desarrollo Rural 2014–2020”, GO TECNOGAR, and by Comunidad de Madrid, through IMIDRA” FP22-ValvaGAR.

REFERENCES

- [1] J. Gai, L. Tang, L., and B. L. Steward, "Automated crop plant detection based on the fusion of color and depth images for robotic weed control," *Journal of Field Robotics*, vol. 37, no. 1, pp. 35-52, 2020.
- [2] J. D. Pujari, R. Yakkundimath, and A. S. Byadgi, "Image processing based detection of fungal diseases in plants," *Procedia Computer Science*, vol. 46, pp. 1802-1808, 2015.
- [3] N. Zhang, et al., "A review of advanced technologies and development for hyperspectral-based plant disease detection in the past three decades," *Remote Sensing*, vol. 12, no. 19, pp. 3188, 2020.
- [4] J. Zhang, et al., "Monitoring plant diseases and pests through remote sensing technology: A review," *Computers and Electronics in Agriculture*, vol. 165, pp. 104943, 2019.
- [5] N. K. Gogoi, B. Deka, and L. C. Bora, "Remote sensing and its use in detection and monitoring plant diseases: A review," *Agricultural Reviews*, vol. 39, no. 4, pp. 307-313, 2018.
- [6] M. Sancho-Adamson, M. I. Trillas, J. Bort, J. A. Fernandez-Gallego, and J. Romanyà, "Use of RGB vegetation indexes in assessing early effects of *Verticillium* wilt of olive in asymptomatic plants in high and low fertility scenarios," *Remote Sensing*, vol. 11, no. 6, pp. 607, 2019.
- [7] A. Yee-Rendon, I. Torres-Pacheco, A. S. Trujillo-Lopez, K. P. Romero-Bringas, and J. R. Millan-Almaraz, "Analysis of New RGB Vegetation Indices for PHYVV and TMV Identification in Jalapeño Pepper (*Capsicum annuum*) Leaves Using CNNs-Based Model," *Plants*, vol. 10, no. 10, pp. 1977, 2021.
- [8] B. D. S. Barbosa, et al. "Application of RGB Images Obtained by UAV in Coffee Farming," *Remote Sensing*, vol. 13, no. 12, pp. 2397, 2021.
- [9] S. Yousfi, J. Marín, L. Parra, J. Lloret, and P. V. Mauri, "Remote sensing devices as key methods in the advanced turfgrass phenotyping under different water regimes," *Agricultural Water Management*, vol. 266, pp. 107581, 2022.
- [10] L. Parra, et al., "Drone RGB images as a reliable information source to determine legumes establishment success," *Drones*, vol. 5, no. 3, pp. 79, 2021.
- [11] L. Parra, D. Mostaza-Colado, J. F. Marin, P. V. Mauri, and J. Lloret, "Methodology to Differentiate Legume Species in Intercropping Agroecosystems Based on UAV with RGB Camera," *Electronics*, vol. 11, no. 4, pp. 609, 2022.
- [12] Z. Iqbal, et al. "An automated detection and classification of citrus plant diseases using image processing techniques: A review," *Comput. Electron. Agr.*, vol. 153, pp. 12-32, 2018.
- [13] J. Boulent, S. Foucher, J. Théau, and P. L. St-Charles, "Convolutional neural networks for the automatic identification of plant diseases," *Frontiers in plant science*, vol. 10, pp. 941, 2019.
- [14] T. Wang, J. A. Thomasson, C. Yang, T. Isakeit, and R. L. Nichols, "Automatic classification of cotton root rot disease based on UAV remote sensing," *Remote Sensing*, vol. 12, no. 8, pp. 1310, 2020.
- [15] U. Shafi, et al. "Wheat rust disease detection techniques: a technical perspective," *Journal of Plant Diseases and Protection*, pp. 1-16, 2022.
- [16] A. Loladze, F. A. Rodrigues Jr, F. Toledo, F. San Vicente, B. Gérard, and M. P. Boddupalli, "Application of remote sensing for phenotyping tar spot complex resistance in maize," *Frontiers in Plant Science*, vol. 10, pp. 552, 2019.
- [17] F. Cao, et al. "Fast detection of sclerotinia sclerotiorum on oilseed rape leaves using low-altitude remote sensing technology," *Sensors*, vol. 18, no. 12, pp. 4464, 2018.
- [18] Q. Liu, et al. "Information fusion of hyperspectral imaging and electronic nose for evaluation of fungal contamination in strawberries during decay," *Postharvest Biol. Technol.*, vol. 153, pp. 152–160, 2019.
- [19] C. Zhang, W. Chen, and S. Sankaran, "High-throughput field phenotyping of *Ascochyta* blight disease severity in chickpea," *Crop Protection*, vol. 125, pp. 104885, 2019.
- [20] S. Azimi, T. Kaur, and T. K. Gandhi, "Water stress identification in chickpea plant shoot images using deep learning," *The 17th India Council International Conference (INDICON)*, Delhi, India, 10-13 Decembre 2020, pp. 1-7.
- [21] S. Azimi, T. Kaur, and T. K. Gandhi, "BAT optimized CNN model identifies water stress in chickpea plant shoot images," *In the 25th International Conference on Pattern Recognition (ICPR)*, Milano, Italy, 10-15 January 2021 pp. 8500-8506.